Characterization of Melanin-TiO_2 Complexes Using FT-IR and ^{13}C Solid-state NMR Spectroscopy

Tae-Joon Park, Jinsoo Kim,†,* Tae-Kyung Kim,† Hee-Moon Park,† Sung-Sup Choi, and Yongae Kim*

*Department of Chemistry, Hankuk University of Foreign Studies, Yongin 449-791, Korea. *E-mail: yakim@hufs.ac.kr*
†New Chemistry Research Division, Korea Research Institute of Chemical Technology, Daejeon 305-343, Korea
†E-mail: jinsoo@krict.re.kr
Received January 10, 2008

The melanin plays key roles to protect internal tissues against the harmful effects of ultraviolet rays in human beings. The most common form of biological melanin is a complex polymer of either or both of 5,6-indolequinone and 5,6-dihydroxyindole carboxylic acid. Micronized TiO_2 has been also widely used as a representative inorganic pigment for the formulation of the UV-care cosmetic products. We synthesized a number of new organic-inorganic nanohybrid compounds to develop sunscreens having stronger UV protecting synergy effects from the sun for the first time. We characterized novel organic-inorganic nanohybrid compounds by $^1H/^{13}C$ cross-polarization magic angle spinning (CPMAS) solid-state NMR and FT-IR spectroscopy. The complexes A, B, and C, simple mixing of the L-DOPA bearing catechol unit with TiO_2 nanoparticle does not show forming covalently bonded organic-inorganic nanohybrid compounds. On the contrary, the complexes D, E, and F show that the line shape changes and chemical shifts of phenoxy carbons of catechol move downfield upon forming the catecholate with Ti (IV). Relationship between the composition of organic-inorganic hybrid and SPF improvements will be studied more in detail in the near future.

Key Words : Solid-state NMR, CPMAS-TOSS, Melanin, Organic/inorganic nanohybrid, UV-protection

Introduction

Melanin is a well-known and the most primitive and universal pigment in living organisms. Melanin brings many benefits to human beings. One of the most recognized benefits is the natural protection against the harmful effects of ultraviolet rays or high frequency light from the sun.[1-5] Although the details of the polymerization in the natural melanin complex are not known, the widespread belief is that melanin has highly polycyclic cross-linked structures consisting of organic precursor molecules such as 5,6-indolequinone and 5,6-dihydroxyindole carboxylic acid as the basic building blocks, as shown in Figure 1. These precursor molecules are derived from the oxidation and polymerization of various organic molecules including L-3,4-dihydroxyphenylalanine (L-DOPA), tyrosine, and cysteine.[6-9] Melanin also displays a strong binding affinity for metal ions such as Cu(II) and Zn(II) because its organic precursor molecules have a catechol moiety, as shown in Figure 1.[10-16] In the meanwhile, titanium dioxide (TiO_2) is a well-known inorganic pigment affording protection from UV degradation. TiO_2 pigments are used in many white or colored products including foods, UV skin protection products, ceramics, rubber products and more because they have a remarkably high reflectance and are inert, thermally stable, non-flammable and non-toxic. Especially, micronized rutile TiO_2 pigments have been widely used for the formulation of UV-care cosmetic products.[17] Inorganic and organic surface treatments for TiO_2 pigments lead to the enhancement of their physical and chemical stability as well as the dispersion stability of the sunscreen dispersion formula.[18-20] Moreover, the chelation of anatase TiO_2 by catechol is a widely known phenomenon as shown in Figure 2.

In this study, we tried to synthesize organic-inorganic nanohybrid compounds using catecholate-Ti(IV) chelation chemistry in order to develop sunscreens with the advantages of both organic materials such as the precursor molecules of melanin and inorganic materials without sacrificing safety and stability in the cosmetic formulation.[21] Characteristic and spectroscopic studies of these newly synthesized organic-inorganic nanohybrid compounds were hampered

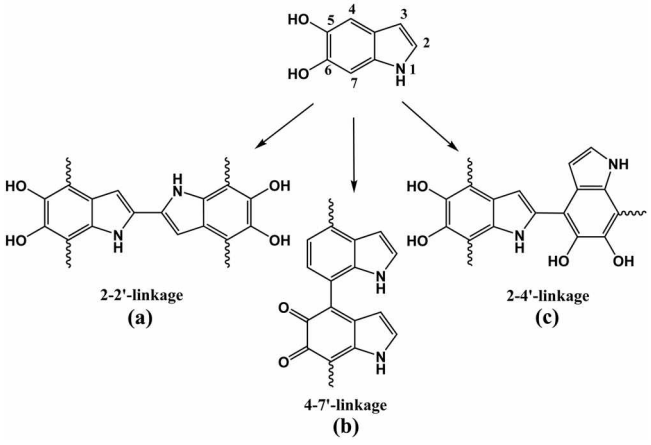

Figure 1. Three types of cross-linkages for the 5,6-dihydroxyindole units are found within the melanin structures as follows; (a) cross-linkages between pyrrole rings (b) chain cross-linkages through benzene-type rings alone (c) branching cross-linkages between benzene and pyrrole rings causing a branch from the main chain. The continuation of the polymer chain is indicated by wavy lines.[9]

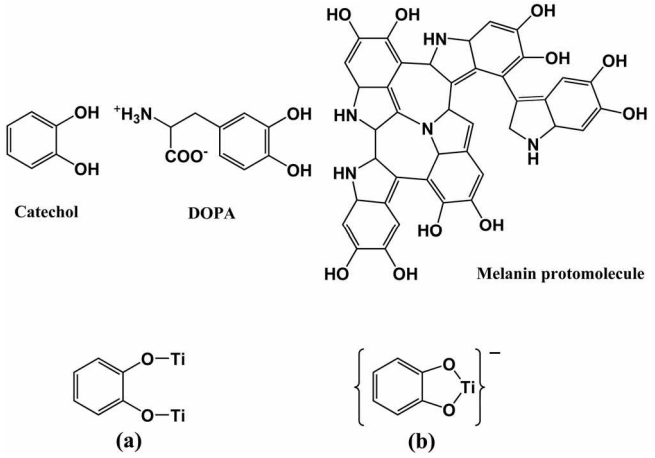

Figure 2. Molecular structures of catechol, DOPA, and melanin protomolecule are shown. The possible binding mechanisms of catechol adsorbed on TiO_2 are shown in (a) bidentate binuclear and (b) bidentate mononuclear.

by their insolubility. Therefore, the structures and properties of the synthetic nanohybrid compounds were characterized by the $^1H/^{13}C$ cross-polarization magic angle spinning with total sideband suppression (CPMAS-TOSS) solid-state NMR spectroscopy, Fourier-transform infrared (FT-IR) spectroscopy, and TEM (data not shown). Especially, $^1H/^{13}C$ CPMAS-TOSS solid-state NMR spectroscopy was mainly used to identify the structures of synthesized organic-inorganic nanohybrid compounds and gave important molecular structural information for binding sites.

Experiments

The TiO_2 used in this experiment was ST-495M rutile nanoparticles from Titan Kogyo in Japan. L-DOPA, catechol, and $Ti(O)SO_4$ (Aldrich, USA) were used as received. Water was purified with a Milli-Q water system (resistivity = 18 Ω cm^{-1}).

Complexes A, B, and C: Three kinds of nanohybrid compounds were provided by COTDE Inc. (Korea). The detail composition of their chemical components is presented in Table 1. All of the components were mixed in deionized water and stirred at 100 rpm at 37 °C for 30 minutes. This process was followed by filtration, washing, and vacuum drying.

Complex D (Catechol-Ti(IV) complex): A freshly prepared 6% aqueous solution of catechol was added to a 10 mmol solution of $Ti(O)SO_4$ in diluted H_2SO_4 at room temperature. After the complete consumption of catechol that took about 1 day and determined by thin layer chromatography, the resultant dark brown solution was treated with an 8 N NaOH aqueous solution to bring the pH up to 3.0. The brown precipitate was filtered, washed and vacuum dried.

Complex E (L-DOPA-Ti(IV) complex): 10 mmol solution of $Ti(O)SO_4$ was diluted with 20 mL of deionized water. 10 mmol of L-DOPA was added slowly with stirring to this solution. After the complete consumption of L-DOPA that took about 1 day and determined by thin layer chromatography, the resultant dark brown solution was treated with an 8 N NaOH aqueous solution to bring the pH up to 3.0. The brown precipitate formed was filtered, washed and vacuum dried.

Complex F (DOPA-melanin-TiO_2 complex): The synthetic melanin was prepared by an L-DOPA air-oxidation method.[16,22] The synthesis of DOPA-melanin was confirmed by comparing its infrared and $^1H/^{13}C$ CPMAS-TOSS NMR spectra with the previously reported one.[22] In order to chelate the catechol functional group of the synthetic DOPA-melanin to the surface of TiO_2, the DOPA-melanin aqueous solution was simply mixed with the TiO_2 nanopowder and dried. 1 L of an aqueous suspension of 25.3 mmol L-DOPA was added drop-wise to a 1 N NH_4OH aqueous solution until pH ~9 was attained. The mixture was maintained under stirring while a continuous stream of air was bubbled through it. The pH was controlled during the reaction time with the successive addition of NH_4OH solution. After 4 days, 5 g of TiO_2 powder was added to one fifth of the synthetic DOPA-melanin aqueous solution. After stirring for an additional 30 min., most of the water was removed under a vacuum rotary evaporator at 30 mmHg and 55 °C) and the residue was completely vacuum dried.

FT-IR spectroscopy was carried out with a FTS-165 Dizilab, BIO-RAD (USA) spectrometer. The IR spectra of the sample were obtained using a KBr pellet prepared with a press after careful grinding of each sample with KBr. The spectral width was 400-4000 cm^{-1} and the spectral resolution was 8 cm^{-1}. Each spectrum was acquired by performing 32 scans.

The solid-state $^1H/^{13}C$ CPMAS-TOSS NMR spectra of all of the compounds were collected using a unity*INOVA* wide bore solid-state NMR spectrometer (Varian, USA) with a magnetic field of 9.4 Tesla operating at a ^{13}C Larmor frequency of 104.21 MHz. ^{13}C NMR experiments were carried out using a 4-mm triple resonance CPMAS probe (T3 probe Varian, USA). In the $^1H/^{13}C$ CPMAS-TOSS experiments, the Hartmann-Hahn polarization transfer with a contact time of 1 ms was optimized to operate at B_1 field strengths of 62.5 kHz and 56.8 kHz for the ^1H and ^{13}C channels, respectively.[23] ^1H CW decoupling power was applied at radiofrequency amplitude of 62.5 kHz during the acquisition period of 40.9 ms.

All of the samples were ground with a mortar and pestle and then packed in a 4-mm zirconium oxide rotor. All of the measurements were taken at ambient temperature of 20 to 24 °C. The magic angle was adjusted using the ^{79}Br resonance of KBr, and all CPMAS-TOSS measurements were carried out at a MAS frequency of 5 kHz. The ^{13}C chemical shifts were externally referenced to the carboxyl signal of glycine at 176.04 ppm and the spectral resolution was 0.01 ppm.

Results and Discussion

Complexes A, B and C. Three kinds of nanohybrid compounds were synthesized according to the compositions

Table 1. Composition of chemical components and SPF of complexes A, B, and C

Sample	Composition of Chemical components (wt%) in H_2O						SPF *in vitro*
	TiO_2	DOPA	Cysteine	Resorcinol	N-acetyl tyrosine	H_2O_2	
TiO_2	10.0	–	–	–	–	–	15
Complex A	10.0	2.0	–	–	1.0	0.2	38
Complex B	10.0	2.0	1.0	1.0	1.0	0.2	28
Complex C	10.0	2.0	3.0	–	1.0	0.2	35

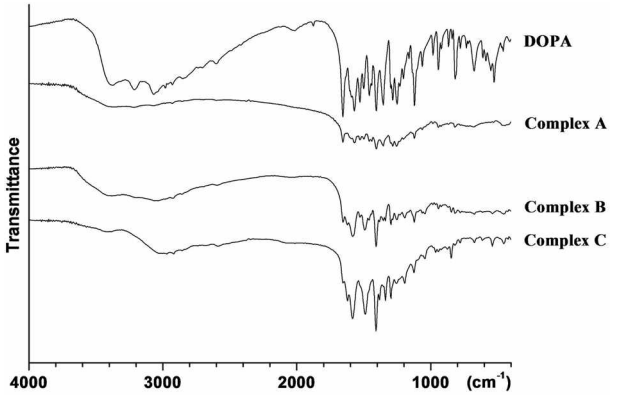

Figure 3. FT-IR spectra of DOPA, complex A, complex B, and complex C. FT-IR spectroscopy was carried out with a FTS-165 Dizilab, BIO-RAD (USA) spectrometer. Each spectrum was acquired by performing 32 scans.

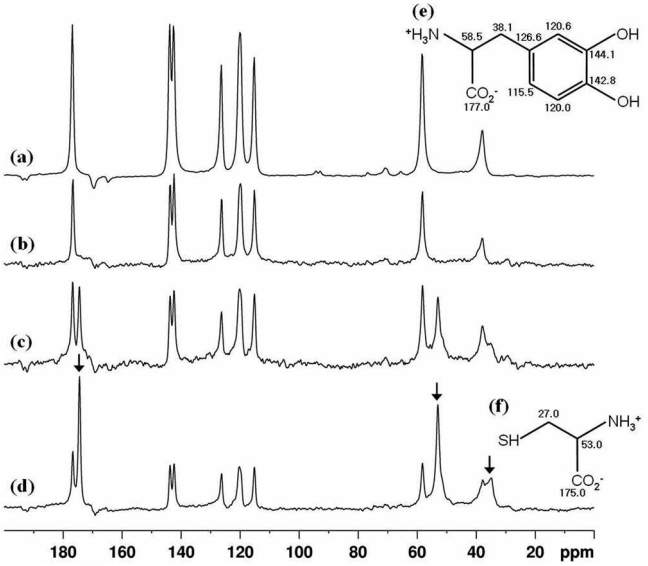

Figure 4. $^1H/^{13}C$ CPMAS-TOSS solid-state NMR spectra of (a) L-DOPA, (b) complex A, (c) complex B, (d) complex C. The isotropic chemical shifts of L-DOPA and cysteine in solution NMR are shown in (e) and (f), respectively. The arrows indicate the shifted resonances originating from cysteine.

of chemical components shown in Table 1. There are some differences in the compositions of cysteine and resorcinol. As shown in Table 1, all of the compounds displayed a high solar protection factor (SPF) which was approximately twice that of TiO_2 itself *in vitro*. The FT-IR spectra are shown in Figure 3. The spectra of complexes A, B, and C are similar to that of L-DOPA with minor changes. The $^1H/^{13}C$ CPMAS-TOSS NMR spectra are shown in Figure 4. The ^{13}C chemical shift assignments in Table 2 were determined on the basis of isotropic chemical shifts of L-DOPA and cysteine which are shown in Figure 4 (e) and (f) respectively.

Primarily, hydrogen peroxide was introduced to convert the L-DOPA and N-acetyl tyrosine to the eumelanin and secondly cysteine was added to mimic the pheomelanin.[24] Resorcinol was compared to the L-DOPA in terms of the ligation ability. All resonances of L-DOPA, N-acetyl tyrosine, and resorcinol were matched very well and easily assigned based on their isotropic chemical shifts in solution NMR spectra. This result means that these compounds are physically mixed with TiO_2 without any chemical reaction either oxidative melanin formation or covalent formation between organic compounds and TiO_2. However, the resonances of cysteine were quite different from the isotropic chemical shifts based on solution NMR spectroscopy. The chemical shifts of carbonyl carbon and a-carbon of cysteine were shifted slightly from 175.0 to 174.4 ppm and 53.5 to 53.4 ppm, respectively. But the ethylene carbon exhibited a relatively large downfield shift from 27.0 to 35.0 ppm. Unlike L-DOPA and N-acetyl tyrosine, cysteine may be chemically reacted with the TiO_2 surface rather than simple physical mixing. No significant quantitative correlation, however, was observed between the composition of the organic-inorganic nanohybrid and the improvement of the SPF. This will be studied in more detail in the future. It is expected that the formation of covalent bond between organic compound and TiO_2 would provide the long term stability of SPF increment. Covalent bond formation of the catechol unit of L-DOPA and melanin with TiO_2 was proved according to the following results of complexes D, E, and F. However, resorcinol which is a geometrical isomer of catechol was not able to form the covalent bond with TiO_2 under the same condition. The same phenomenon was also observed in the case of hydroquinone.

Complex D: Catechol-Ti(IV) complex. Figure 5(a) show the $^1H/^{13}C$ CPMAS-TOSS NMR spectra of complex D in comparison with that of catechol in Figure 5(b). The ^{13}C chemical shift assignments are based on isotropic chemical shifts of solution NMR and summarized in Table 3. The spectrum of catechol-Ti(IV) complex shows broader resonances than that of catechol itself. This means that the catechol in catechol-Ti(IV) complex has slower motion than crystalline form of catechol itself. This is a direct evidence for forming complex. The downfield shift of 142.5 to 154.2 ppm for the diphenolic phenoxy carbons of complex D can

Table 2. ^{13}C chemical shift resonances determined by CPMAS-TOSS solid-state NMR

Sample	Carbonyl	Diphenolic phenoxy	Aromatic and Indolic	Aliphatic
L-DOPA	177.0	142.8, 144.1	115.5, 120.0, 120.6, 126.6	38.1, 58.5
Complex A	177.0	142.8, 144.1	115.5, 120.0, 120.6, 126.6	38.1, 58.5
Complex B	177.0, 174.4	142.8, 144.1	115.5, 120.0, 120.6, 126.6	35.0, 38.1, 53.4, 58.5
Complex C	177.0, 174.4	142.8, 144.1	115.5, 120.0, 120.6, 126.6	35.0, 38.1, 53.4, 58.5

The chemical shifts are in units of ppm referenced to the glycine carboxyl resonance at 176.04 ppm.

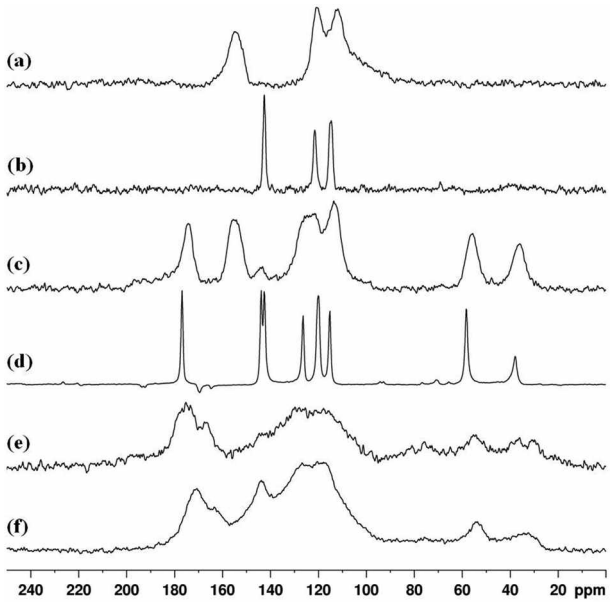

Figure 5. $^{1}H/^{13}C$ CPMAS-TOSS solid-state NMR spectra of (a) complex D, (b) catechol, (c) complex E, (d) L-DOPA, (e) complex F, and (f) melanin. All spectra were acquired using CPMAS-TOSS pulse sequence with 1 ms mixing time, recycle delay of 3 s, spinning at 5 kHz, and the $\pi/2$ pulse width for ^{1}H is 4.2 s. The experimental parameters are the same for all of the spectra.

be explained that phenoxy carbons are binding site upon the formation of complex D as shown in Figure 2. Figure 6(a) shows the FT-IR spectra of complex D in comparison with that of catechol in Figure 6(b). The appearance of strong absorption bands at 1478 and 1258 cm^{-1} confirms that catechol binds to the oxide surfaces in the bidentate dianion form (Figure 2(a)).[15]

Complex E: L-DOPA-Ti(IV) complex. Figure 5(c) shows the $^{1}H/^{13}C$ CPMAS-TOSS NMR spectra of complex E in comparison with that of L-DOPA in figure 5(d) and the chemical shifts of their corresponding carbons are summarized in Table 3. The spectrum of L-DOPA-Ti(IV) complex also shows broader resonances than that of L-DOPA itself. This also means that the L-DOPA in L-DOPA-Ti(IV) complex has slower motion than crystalline L-DOPA itself. This is a direct evidence for forming complex. The disappearance of the chemical shifts 144.1 ppm related to the diphenolic phenoxy carbons and the new signals which appeared in the region of 154.0 ppm confirm the formation of the catecholate-Ti(IV) complex. The signals for the carbonyl carbon and aliphatic carbons of complex E appear at a higher field compared to those of L-DOPA. It means that the interaction between the α-amino acid group of L-DOPA and Ti(IV) are also existed. Figure 6(c) shows the FT-IR spectra of complex E in comparison with that of L-DOPA in Figure 6(d). The strong absorption bands at 1486 and 1268 cm^{-1} can be assigned to the chelation of catechol to Ti(IV). The carbonyl stretching band (1663 cm^{-1}) of the carboxylic acid in L-DOPA disappeared upon the formation of complex E. This suggests the binding of Ti(IV) at the amino acid site of L-DOPA under the strong acid conditions.

Complex F: DOPA-melanin-TiO_2 complex. Figure 5(e) shows the $^{1}H/^{13}C$ CPMAS-TOSS NMR spectra of complex F in comparison with that of the synthetic DOPA-melanin in Figure 5(f). The spectrum of DOPA-melanin already shows broader resonances because of its higher molecular weight and highly polycyclic cross-linked structure. The most dominant spectral difference is the carbonyl carbon isotropic resonance near 170 ppm to aromatic carbon resonances near 143 ppm and 120 ppm ratio.

The signal for the aromatic carbon bearing oxygen in 143.9 ppm of the synthetic melanin appears to be decreased and even almost disappeared. In addition, aromatic carbon resonances of synthetic DOPA-melanin show fairly well resolved resonances at 143.9 ppm and centered at 123.0 ppm, whereas in complex F only a single featureless signal centered at approximately 130 ppm. Therefore, diphenolic phenoxy carbon resonances near 143.9 ppm almost dis-

Table 3. ^{13}C chemical shift resonances determined by CPMAS-TOSS solid-state NMR

Sample	Carbonyl	Diphenolic phenoxy	Aromatic and Indolic	Aliphatic
Complex D	–	154.2	112.9, 121.1	–
Catechol	–	142.5	114.9, 121.5	–
Complex E	172.2	141.3, 154.0	110.8, 119.3, 122.8	33.5, 53.3
L-DOPA	177.0	142.8, 144.1	115.5, 120.0, 120.6, 126.6	38.1, 58.5
Complex F	175.5, 167.6	143.6 (very weak)	127.5, 119.0	34.8, 54.5
Melanin	170.9, 163.5	143.9	127.5, 119.0	32.5, 54.3

The chemical shifts are in units of ppm referenced to the glycine carboxyl resonance at 176.04 ppm

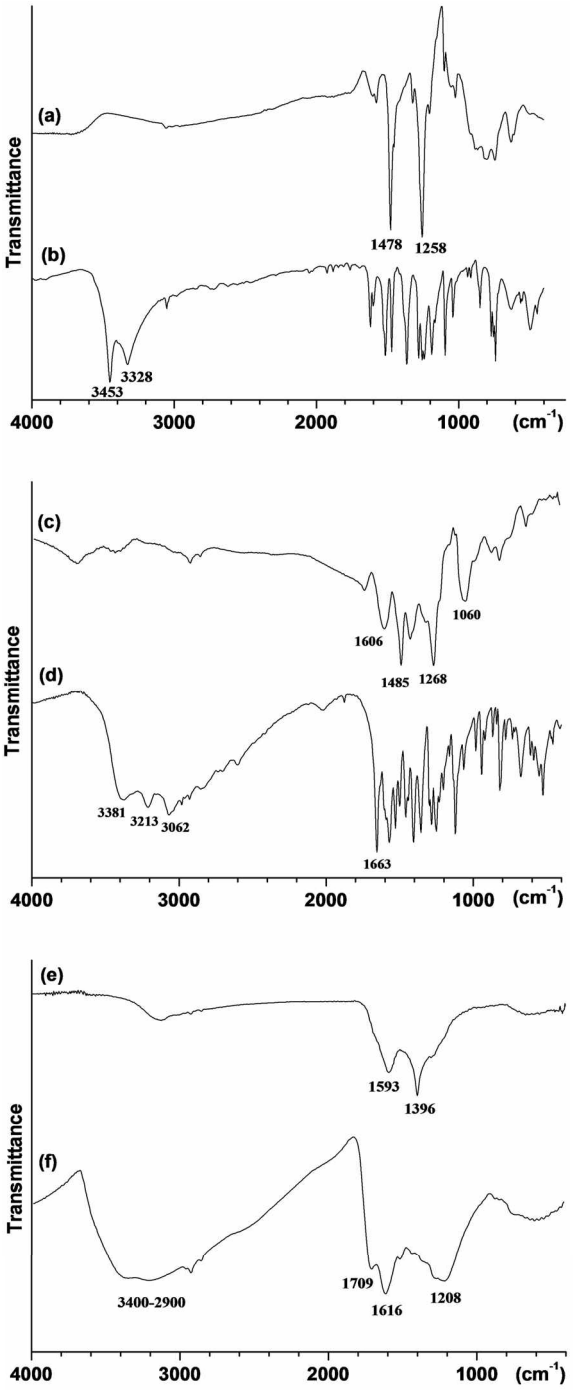

Figure 6. FT-IR spectra of (a) complex D, (b) catechol, (c) complex E, (d) L-DOPA, (e) complex F, and (f) melanin. FT-IR spectroscopy was carried out with a FTS-165 Dizilab, BIO-RAD (USA) spectrometer.

appear with an increase of chemical heterogeneity in complex F. Although less evident, these changes were also described forming the melanin catecholate complex in the case of complex F.[25] Figure 6(e) shows the FT-IR spectra of complex F in comparison with that of melanin in Figure 6(f). The free dihydoxyphenolic OH stretching band at 3400-2900 cm^{-1} of DOPA-melanin doesn't exist any longer in the spectrum of the DOPA-melanin-TiO_2 complex F (Figure 6(e)). These support the formation of the melanin catecholate complex on the surface of TiO_2.

Conclusions

In this study, new organic-inorganic nanohybrid compounds were successively synthesized and characterized by FT-IR and ^{13}C solid-state NMR spectroscopy with the goal of developing new sunscreens. Even though infrared spectroscopy is also quite useful for the analysis of solid materials, because it can be performed on small amounts of the solid substance with relatively easy operation, it is insufficient to confirm the molecular structural details of the chemical bonds and chemical conformations at the atomic level. Therefore, we demonstrated the use of $^{1}H/^{13}C$ CPMAS-TOSS solid-state NMR spectroscopy[26-28] as a simple and very powerful tool for the investigation of the chelation of the catechol species with Ti(IV). Complexes A, B, and C, simple mixing of the L-DOPA bearing catechol unit with TiO_2 nanoparticle does not form the covalently bonded organic-inorganic nanohybrid compound. The $^{1}H/^{13}C$ CPMAS-TOSS solid-state NMR spectra of complexes D, E, and F show that the line shape and chemical shifts of the phenoxy carbons of catechol change upon forming the catecholate with Ti (IV). Even though L-DOPA and DOPA-melanin are more complicated systems that have more functional groups and highly polycyclic cross-linked structure, we propose the first observation of L-DOPA-Ti (IV) and DOPA-melanin-TiO_2 complexes that have a catecholic subunit in common. Further work is in progress in order to establish an efficient method of preparing melanin-TiO_2 complexes and develop novel UV shielding raw materials.

Acknowledgments. This work was supported by the GRRC Program of Gyeonggi Province [PRO7023, Development of Anti-Bacterial Peptides Using Lactophorin] and the HUFS Research Fund of 2007. J. Kim was supported by KRICT Research Fund of KK-0603-KO and KK-0703-CO.

References

1. Chedekel, M. R.; Fitzpatrick, T. B.; Zeise, L. *Melanin: Its Role in Human Photoprotection*; Valdenmar Publishing Company: 1995; pp 11-12.
2. Kolias, N. S. R.; Zeise, L.; Chedekel, M. R. *J. Photochem. Photobiol. B: Biol.* **1991**, *9*, 135.
3. Moire, C.; Deflandre, A.; Junino, A.; Goetz, N. *Abstr. 3rd Annual Meeting of the European Society for Pigment Cell Research*; Amsterdam, 1991; p 39.
4. Scalia, M.; Geremia, E.; Corsaro, C.; Sautoro, C.; Baretta, D.; Sichel, G. *Pigm. Cell Res.* **1990**, *3*, 115.
5. Pathak, M. S.; Jimbow, K.; Szabo, G.; Fitzpatric, T. B. *Photochem. Photobiol. Rev.* **1976**, *2*, 211.
6. Prota, G. *Melanins and Melanogenesis*; Academic Press: Sandiego, 1992; pp 152-290.
7. Crippa, R.; Horak, V.; Prota, G.; Svoronos, P.; Wolfram, L.; Brossi, A. *Alkaloids*; Academic Press: New York, 1989; pp 253-323.
8. Riley, P. A. *Int. J. Biochem. Cell Biol.* **1997**, *29*, 1235.
9. Aime, S.; Fasano, M.; Bergamasco, B.; Lopiano, L.; Quattrocolo,

G. *Adv. Neurol.* **1996**, *69*, 263.
10. Blesa, M. A.; Weisz, A. D.; Morando, P. J.; Salfity, J. A.; Magaz, G. E.; Regazzoni, A. E. *Coord. Chem. Rev.* **2000**, *196*, 31.
11. Rodriguez, R.; Blesa, M. A.; Regazzoni, A. E. *J. Coll. and Inter. Sci.* **1996**, *177*, 122.
12. Borgias, B. A.; Cooper, S. R.; Koh, Y. B.; Raymond, K. N. *Inorg. Chem.* **1984**, *23*, 1009.
13. Connor, P. A.; Dobson, K. D.; McQuillan, A. J. *Langmuir* **1995**, *11*, 4193.
14. Moser, J.; Punchihewa, S.; Infelta, P. P.; Grätzel, M. *Langmuir* **1991**, *7*, 3012.
15. Martin, S. T.; Kesselman, J. M.; Park, D. S.; Lewis, N. S.; Hoffman, M. R. *Environ. Sci. Technol.* **1996**, *30*, 2535.
16. Stainsack, J.; Mangrich, A. S.; Maia, C. M. B. F.; Machado, V. G.; Santos, J. C. P.; Nakagaki, S. *Inorg. Chim. Acta* **2003**, *356*, 243.
17. Christ, R. W. *Cos. & Toil. Mag.* **2003**, *118*, 73.
18. Monte, S. J.; Island, S.; Bruins, P. F. *U. S. Patent, 4, 098, 758*, 1978.
19. Schlossman, D. S.; Orange, W. *U. S. Patent, 5, 356, 617*, 1994.
20. Kim, J. W.; Shim, J. W.; Bae, J. H.; Han, S. H.; Kim, H. K.; Chang, I. S.; Kang, H. H.; Suh, K. D. *Colloid Polym. Sci.* **2002**, *280*, 584.
21. Jang, D. I. *Korea Patent, 0084598*, 2004.
22. Aime, S.; Crippa, P. R. *Pigm. Cell Res.* **1988**, *1*, 355.
23. Hartmann, S. R.; Hahn, E. L. *Phys. Rev.* **1962**, *128*, 2043.
24. Giuseppe, P. *Pigm. Cell Res.* **2000**, *13*, 283.
25. Ghiani, S.; Baroni, S.; Burgio, D.; Digilio, G.; Fukuhara, M.; Martino, P.; Monda, K.; Nervi, C.; Kiyomine, A.; Aime, S. *Magn. Reson. Chem.* **2008**, *46*, 471.
26. Kim, Y.; Kim, A. *Bull. Kor. Chem. Soc.* **2002**, *23*, 1729.
27. Kim, Y. *Bull. Kor. Chem. Soc.* **2003**, *24*, 1281.
28. Kim, Y. *Bull. Kor. Chem. Soc.* **2006**, *27*, 386.